Selective area growth and characterization of InGaN nano-disks implemented in GaN nanocolumns with different top morphologies

S. Albert,[1,a)] A. Bengoechea-Encabo,[1,a)] P. Lefebvre,[1,2] F. Barbagini,[1] M. A. Sanchez-Garcia,[1] E. Calleja,[1] U. Jahn,[3] and A. Trampert[3]
[1]*ISOM and Departamento de Ingeniería Electrónica, ETSI Telecomunicación, Universidad Politécnica de Madrid, Ciudad Universitaria s/n, 28040 Madrid, Spain*
[2]*CNRS–Laboratoire Charles Coulomb (L2C), UMR5221, F-34095 Montpellier, France*
[3]*Paul-Drude-Institut für Festköperelektronik, Hausvogteiplatz 5-7, 10117 Berlin, Germany*

(Received 25 April 2012; accepted 23 May 2012; published online 5 June 2012)

This work reports on the morphology control of the selective area growth of GaN-based nanostructures on c-plane GaN templates. By decreasing the substrate temperature, the nanostructures morphology changes from pyramidal islands (no vertical m-planes), to GaN nanocolumns with top semipolar r-planes, and further to GaN nanocolumns with top polar c-planes. When growing InGaN nano-disks embedded into the GaN nanocolumns, the different morphologies mentioned lead to different optical properties, due to the semi-polar and polar nature of the r-planes and c-planes involved. These differences are assessed by photoluminescence measurements at low temperature and correlated to the specific nano-disk geometry. © *2012 American Institute of Physics*. [http://dx.doi.org/10.1063/1.4728115]

Group III-nitride semiconductors are widely used nowadays in optoelectronic devices, in particular, InGaN alloys for light emitters working in the whole visible spectral region,[1–3] as well as for white light generation. Most of the efforts devoted to these materials focused on c-plane oriented, two-dimensional quantum well (QW) structures. However, the performance of these planar structures is limited by: (i) the reduction of the radiative recombination rate induced by the quantum confined Stark effect due to spontaneous and piezoelectric polarizations and (ii) the high density of non-radiative defects due to the increasing lattice mismatch between GaN and InGaN alloys with higher In content. The growth of high quality InGaN alloys with In content above 25% poses big challenges derived from the quite different optimal growth temperatures for GaN and InN. Heteroepitaxy of InGaN/GaN QWs on sapphire, Si, or SiC is particularly prone to suffer from the above mentioned problems. On the other hand, it has been shown that dislocation- and strain free III-nitrides can be grown on Si(100) and (111), as well as on amorphous SiO_2 substrates[4–8] by forming quasi one-dimensional structures such as self-assembled nanocolumns (NCs).

White LEDs based on InGaN/GaN self-assembled nanocolumnar structures have been demonstrated, showing multicolor emission derived from an inhomogeneous distribution of In due to either changes in NCs diameter (that affect the axial growth rate); axial and radial strain variations, or the inherent tendency of InGaN alloys to have composition fluctuations.[9,10] Although self-assembled NCs are easy to grow with a high crystal quality that favors the study of basic material properties, efficient LEDs based on self-assembled NCs suffer severe limitations derived from a strong dispersion (morphological, electrical) inherent to the self-assembled process. Problems of dark spots generated at defective NCs (crystal defects upon NCs merging) and/or an inhomogeneous current injection may derive in a poor electroluminescence (EL) yield.[11]

During the last years, selective area growth (SAG) of GaN (Refs. 12–15) has been developed to grow NCs with well-controlled position and diameter, resulting in geometrical arrays of NCs with very little morphology dispersion. In the case of SAG of GaN NCs on c-plane GaN templates, the growth front (topside) is generally formed by semi-polar planes (r-planes) and a topmost c-plane ("pencil-like" profile).[12–15] As a result, InGaN quantum disks (QDisk) embedded within the GaN NC follow similar profiles.[14]

In this work, ordered GaN NCs with and without InGaN nano-disks, i.e., an InGaN insertion with a thickness between 10 and 25 nm, have been grown by plasma-assisted molecular-beam epitaxy (PAMBE) at different temperatures in order to study the change in morphology and its influence on the optical properties of these nanostructures.

The PAMBE system used in this work was equipped with a rf-plasma source providing active nitrogen and standard Knudsen cells for Ga and In. The sample temperature was controlled and monitored by a thermocouple located on the heater stage. All samples were grown using nanohole titanium masks fabricated by e-beam lithography (EBL) on commercial (0001) GaN templates grown on sapphire (Lumilog). Details of the mask preparation can be found elsewhere.[15] After a standard degreasing, the substrates were out gassed for 30 min at 300 °C. The molecular fluxes were calibrated in (0001) GaN and (0001) InN growth rate units (nm/min).[16] In wurtzite GaN and InN the areal densities referring to 1 monolayer (ML) are 1.14×10^{15} GaN/cm^2 and 9.17×10^{14} InN/cm^2, respectively.[17,18] After growth the samples were studied by scanning electron microscopy (SEM), low temperature photoluminescence (PL), scanning transmission electron microscopy (STEM), high-angle annular dark field scanning transmission electron microscope (HAADF-STEM), and high resolution transmission electron microscopy (HRTEM). PL was excited with a He-Cd laser at

[a)]S. Albert and A. Bengoechea-Encabo contributed equally to this work.

30 mW. Our PL collection system exhibits some chromatic effects that affect the overall shape of measured spectra, in case of broad PL lines. We chose to optimize the PL collection at the center of the visible spectrum, which may slightly minimize contributions from the red and blue-violet regions.

A first series of ordered NCs were grown during 1 h at 940, 900, and 860 °C, in order to study the effect of temperature on morphology. The gallium (Φ_{Ga}) and nitrogen (Φ_N) fluxes used were 15 nm/min and 5 nm/min, respectively. In order to determine the effect of the Φ_{Ga} (III/V-ratio) on the NCs morphology, a similar sample to that grown in the previous series at 900 °C was grown just changing the gallium flux to $\Phi_{Ga} = 18$ nm/min. To check the morphology impact on the optical properties, a second series of ordered NCs samples, having either pencil-like or flat top, were grown including a single InGaN nano-disk. These nano-disks were grown in all cases at 625 °C with $\Phi_N = 14$ nm/min, $\Phi_{Ga} = 4.3$ nm/min, and $\Phi_{In} = 4.3$ nm/min. The nano-disk was capped with a GaN layer (20–40 nm thick) grown under the same conditions used for the InGaN nano-disk (without In flux).

The main difference in optimal growth conditions when growing GaN NCs by SAG on GaN templates, compared to the self-assembled process on Si(111), is a much higher temperature needed for SAG and, consequently, a much higher III/V ratio needed to balance metal desorption.[15,17] SAG requires a much higher temperature to achieve selectivity, that is, to provide nucleation and growth within each nanohole while avoiding it on the mask. A higher temperature optimizes Ga atoms diffusion into the nanoholes while reducing the possibility that they may bind N atoms while being on the mask.

In terms of selectivity, an increase of the growth temperature acts in opposite way to an increase in the amount of active nitrogen.[17] A higher nitrogen flux increases the probability for GaN formation on the mask because the excess nitrogen favors the Ga-N bonding before Ga ad-atoms desorb or diffuse into a nanohole. In addition, the excess nitrogen increases the energy barrier for Ga adatoms diffusion, which makes the GaN formation on the mask before Ga atoms reach a nanohole even more likely. Both mechanisms lead to a loss of selectivity.[19] On the other hand, an increase in the growth temperature enhances both the Ga adatoms diffusion length on the mask and the Ga desorption rate, thus, improving selectivity.

In addition to selectivity, the substrate temperature also affects critically the growth inside the nanoholes. Considering that an increase of the growth temperature reduces exponentially (by desorption) the Ga amount that reach by diffusion or direct impinging the nanoholes, a high enough growth temperature may suppress or inhibit the vertical growth. Such a case is shown in Fig. 1(a) where ordered GaN (nominally aimed to form NCs) grown with $\Phi_{Ga} = 15$ nm/min, $\Phi_N = 5$ nm/min at 940 °C reveal a perfect selectivity but, instead of NCs, the growth results in GaN pyramids. Once this geometry is reached, the GaN pyramids size and shape does not change when growth goes on.[15] This inhibition of the vertical growth after the initial nucleation stage seems to relate to a lack of sufficient Ga within the nanoholes. In this particular case (Fig. 1(a)) the nominal Φ_{Ga} was not high enough to grow NCs. Nucleation took place because, upon starting growth, a strong Φ_{Ga} transient (shutter opened) yields an initial value higher (20 nm/min) than the nominal one (15 nm/min). This leads to a higher local III/V ratio within the nanohole for a short time, until the transient is over. This mechanism will dominate growth whenever the chosen nominal Φ_{Ga} is too small to keep the vertical growth.

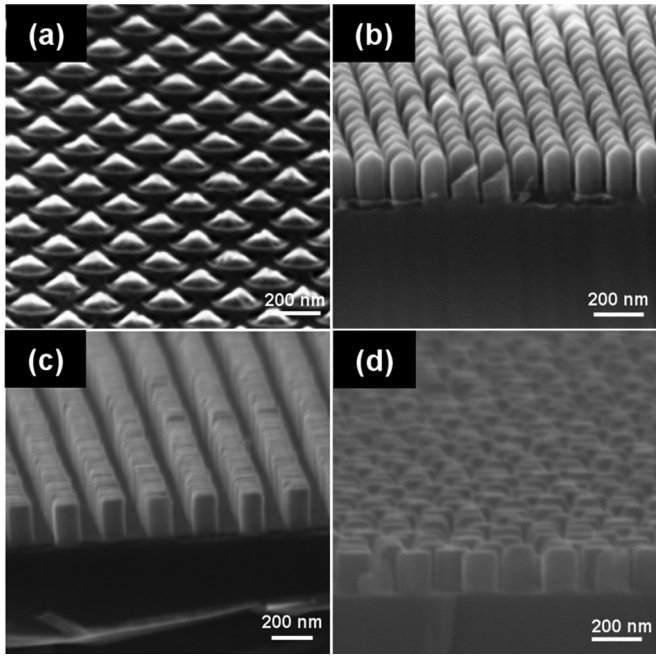

FIG. 1. SEM images of different ordered GaN NC morphologies, grown under the same nominal III/V ratio (=3) but different temperatures; (a) 940 °C, (b) 900 °C, and (c) 860 °C. In (d), flat top ordered GaN NCs grown at 900 °C, like (b), but under a nominal III/V ratio of 3.6.

A new NCs sample was grown keeping the previous nominal Φ_{Ga}, but lowering the temperature from 940 to 900 °C, that is, significantly reducing the Ga desorption rate. These conditions provide an increased Ga amount within the nanoholes leading to vertical growth of ordered NCs, as shown in Fig. 1(b), that still have pyramidal top facets (r-planes).[15] In the first case of suppressed vertical growth and even in the second one (Figs. 1(a) and 1(b)) the growth conditions are most likely N-rich, i.e., Φ_{Ga} limits the growth rate.

A further reduction in the growth temperature down to 860 °C leads to the formation of ordered GaN NCs with a flat top (c-plane), as shown in Fig. 1(c). Based on the above arguments this morphology change can be attributed to an increase of the local III/V ratio within the nanoholes due to a decrease in the Ga desorption rate. In order to verify this interpretation, a sample of ordered GaN NCs was grown at 900 °C with an increased nominal Ga-flux of $\Phi_{Ga} = 18$ nm/min (III/V ratio of 3.6). As shown in Fig. 1(d), the expected morphology change is indeed observed, i.e., a transition from pyramidal (Fig. 1(b)) to flat-top (Fig. 1(d)) by increasing the nominal III/V ratio (impinging Φ_{Ga}). Since this morphology transition depends basically on the increased amount of Ga reaching the nanoholes either by reducing Ga desorption (temperature) or by increasing the nominal impinging Φ_{Ga}, this suggests that a change from N-rich to Ga-rich conditions is involved. It is known that for

homoepitaxial growth of GaN, the layer morphology is determined by the growth regime either Ga-rich or N-rich[20,21] and that N-rich conditions yield a faceted surface.

Another fact that backs this interpretation comes from Ref. 15. In that work, a similar sample as that in Fig. 1(a), grown under similar conditions but on much smaller nanohole sizes, yielded vertical growth of NCs with flat tops. These results are again explained in terms of an increase in local III/V ratio. It can be concluded that the three main parameters controlling the SAG of GaN by MBE in terms of selectivity and morphology are (i) the nominal Φ_{Ga}, (ii) the growth temperature, and (iii) the mask design, all aiming to an adequate local III/V ratio within the nanoholes.

When including InGaN nano-disks into ordered GaN NCs, their morphology is determined by the starting flat or pyramidal top of GaN NCs, as shown by the HAADF-STEM images in Figs. 2(a) and 2(b). For flat top GaN NCs the InGaN nano-disk has parallel (c-plane) interfaces to the GaN beneath and above it (cap layer) showing a true disk geometry. For pyramidal GaN NCs, the InGaN inclusion has parallel interfaces to the existing r-planes of both the GaN beneath and above it (cap). It has to be noted that the nano-disks shown in Figs. 2(a) and 2(b) were grown for 80 and 160 s, respectively. Considering the InGaN thickness as the distance between parallel facets (either c- or r-planes), from the Figs. 2(a) and 2(b) the thickness of the InGaN nano-disk can be estimated to be around 12 nm for the InGaN nano-disk grown on pyramidal top, and 25 nm for the InGaN nano-disk grown on the flat top. In addition, when growing an InGaN nano-disk on pyramidal top GaN NCs, structural defects like stacking faults and even cubic GaN inclusions can be observed on the top GaN cap layer (Figs. 2(c) and 2(d)). These features are most likely due to a too low temperature to grow the GaN cap layer (same as for the InGaN QDisk).

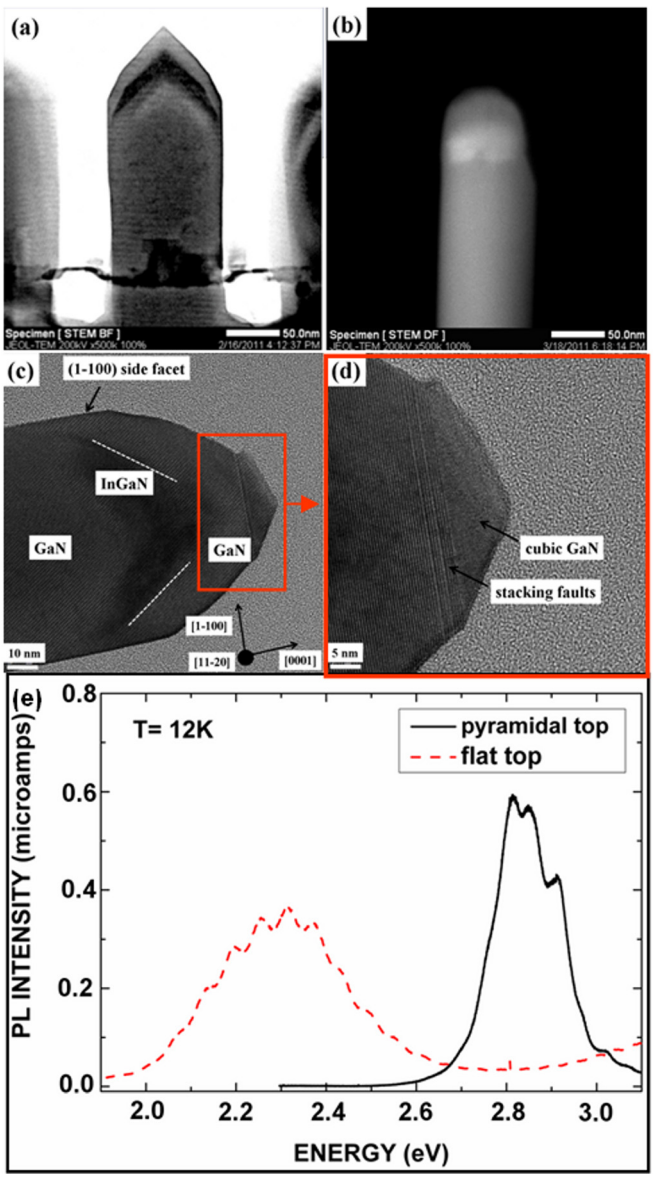

FIG. 2. (a) STEM bright-field image of InGaN QDisk embedded in ordered GaN NCs with pencil like top, (b) HAADF-STEM image of an InGaN QDisk embedded in ordered GaN NCs with flat top, (c), (d) HRTEM images of an InGaN nano-disk embedded shown in (a), (e) low temperature PL measurements of samples shown in (a) and (b).

In Fig. 2(e) the low temperature PL spectra of the InGaN nano-disks shown in Figs. 2(a) and 2(b) reveal a shift of around 0.5 eV of the PL peak positions. In the particular case of these two samples, this shift may, *a priori*, be ascribed to a variety of effects, namely different (i) levels of In incorporation, (ii) strain, (iii) degrees of confinement due to different thicknesses, and (iv) internal electric fields, due to the different polar character of the growth planes (Stark effect).

In order to allow for a better comparison, two more single InGaN nano-disks embedded in either pyramidal or flat tops have been grown. The growth time of the InGaN nano-disk was in both cases 160 s. Based on the results shown in Figs. 2(a) and 2(b) we can assume an InGaN nano-disk thickness of around 25 nm for both samples. The PL spectra shown in Fig. 3 are quite dissimilar regarding both emission intensity and peak energy position. The "pyramidal-shaped" InGaN spectrum reveals a peak centered at around 2.75 eV. On the other hand, the PL spectrum of InGaN nano-disks grown on flat-top GaN NCs shows a line peaking at around 2.32 eV, that is, ~0.4 eV below that observed for "pyramidal-shaped" InGaN. Besides this energy shift, a reduction in the emission intensity by a factor of 43 can be observed for the InGaN nano-disks grown on flat top GaN NCs.

Considering the equivalent thicknesses of 25 nm for the InGaN nano-disks in both samples, differences in confinement

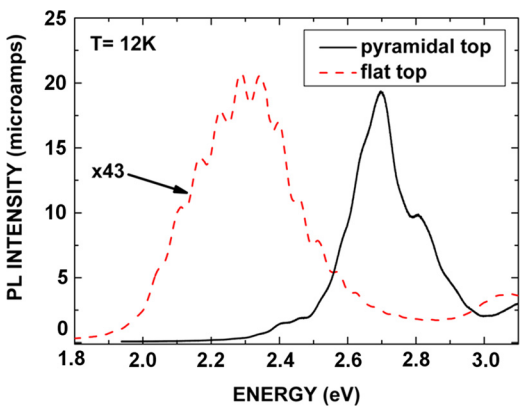

FIG. 3. Low temperature PL spectra of two GaN/InGaN/GaN ordered nanocolumnar heterostructures with the same nominal thickness of the InGaN part.

as a potential explanation for the observed differences in the spectra can be discarded. On the other hand, the different polar character of the growth planes and/or the different strain levels may be considered responsible for the observed energy shift due to the build up of an electric field, in the case of InGaN nano-disks with the c-plane (flat) top. In the latter case, the electric field (spontaneous and/or piezo origin) would lead to the formation of respective triangular potential wells for the electrons and holes at both InGaN/GaN interfaces, separating electron and hole wave functions thus reducing the oscillator strength (intensity) in combination with a red-shift of the emission (Stark effect). The reduced intensity, observed in the case of InGaN nano-disks with c-plane top, might as well be partially caused by the presence of non-radiative defects, as reported for the case of InGaN/GaN QWs.[22] On the other hand, it has been shown elsewhere[23] that semi-polar planes, such as r-planes, undergo a total polarization close to zero, leading to a negligible electric field. At this point it has to be noted that given the usual values encountered for electric fields in c-plane InGaN/GaN quantum wells,[24] the optical transition of a totally strained InGaN nano-disk of the given thickness grown on the flat top should lie in the infrared. Following that, a certain degree of strain relaxation has to be present in the sample studied by PL (Fig. 3).

The possibility that the tip morphology of the NCs has an influence on the indium incorporation during growth cannot be eliminated entirely. However, if it were to be solely due to In composition difference, a shift of 0.4 eV would correspond to a difference of ~0.15–0.16 in indium composition[3] which is unlikely considering that the same growth conditions were used for the growth of InGaN nano-disk in both samples.

In summary, ordered GaN NCs were grown by PAMBE on GaN templates at different substrate temperatures and impinging Φ_{Ga}. Depending on the growth temperature, three growth regimes can be distinguished: (i) GaN pyramids with no further vertical growth, (ii) GaN NCs with a top formed by r-planes, and (iii) GaN NCs with c-plane top surfaces. The effects of the growth temperature and Φ_{Ga} on the NCs morphology have been described in terms of changes in the local III/V ratio within the nanoholes and corroborated by similar morphology changes induced by pure geometrical factors (nanohole size).[15]

The impact of morphology changes, in particular, the polar character of the planes acting as growth front, on the optical properties of InGaN nano-disks has been assessed by PL measurements that show a clear red shift and reduced PL emission intensity for the InGaN nano-disks grown on flat top (c-plane) GaN NCs at low temperature. This shift is interpreted in terms of a stronger Stark effect along polar c-direction.

We acknowledge partial financial support by the EU FP7 Contract SMASH 228999-2; the Initial training network RAINBOW project PITN-GA-2008-213238, the Marie Curie Intra European Fellowship within the 7th European Community Framework, PIEF-GA-2009-253085 and by Spanish projects CAM/P2009/ESP-1503 and MICINN MAT2011-26703.

[1]S. Nakamura, G. Fasol, and S. J. Pearton, *The Blue Laser Diode: The Complete Story* (Springer, Berlin, 2000).
[2]F. K. Yam and Z. Hassan, Superlattices Microstruct. **43**, 1 (2008).
[3]T. Kuykendall, P. Ulrich, S. Aloni, and P. Yang, Nat. Mater. **6**, 952 (2007).
[4]E. Calleja, M. A. Sachnchez-Garcia, F. J. Sanchez, F. Calle, F. B. Naranjo, E. Muñoz, U. Jahn, and K. Ploog, Phys. Rev. B **62**, 16826 (2000).
[5]R. Meijers, T. Richter, R. Calarco, T. Stoica, H. P. Bochem, M. Marso, and H. Lüth, J. Cryst. Growth **289**, 381 (2006).
[6]N. Thillosen, K. Sebald, H. Hardtdegen, R. Meijers, R. Calarco, S. Montanari, N. Kaluza, J. Gutowski, and H. Luth, Nano Lett. **6**, 704 (2006).
[7]M. Yoshizawa, A. Kikuchi, M. Mori, N. Fujita, and K. Kishino, Jpn. J. Appl. Phys. **36**, L459 (1997).
[8]Y. S. Park, C. M. Park, D. J. Fu, T. W. Kang, and J. E. Oh, Appl. Phys. Lett. **85**, 5718 (2004).
[9]K. Kishino, A. Kikuchi, H. Sekiguchi, and S. Ishizawa, Proc. SPIE **6473**, 64730T (2007).
[10]H.-W. Lin, Y.-J. Lu, H.-Y. Chen, H.-M. Lee, and S. Gwo, Appl. Phys. Lett. **97**, 073101 (2010).
[11]A. L. Bavencove, G. Tourbot, J. Garcia, Y. Désières, P. Gilet, F. Levy, B. André, B. Gayral, B. Daudin, and L. S. Dang, Nanotechnology **22**, 345705 (2011).
[12]H. Sekiguchi, K. Kishino, A. Kikuchi, Appl. Phys. Express **1**, 124002 (2008).
[13]K. Kishino, H. Sekiguchi, and A. Kikuchi, J. Crystal Growth **311**, 2063 (2009).
[14]H. Sekiguchi, K. Kishino, and A. Kikuchi, Appl. Phys. Lett. **96**, 231104 (2010).
[15]A. Bengoechea-Encabo, F. Barbagini, S. Fernandez-Garrido, J. Grandal, J. Ristic, M. A. Sanchez-Garcia, E. Calleja, U. Jahn, E. Luna, and A. Trampert, J. Crystal Growth **325**, 89–92 (2011).
[16]B. Heying, R. Averbeck, L. F. Chen, E. Haus, H. Riechert, and J. S. Speck, J. Appl. Phys. **88**, 1855 (2000).
[17]S. Fernández-Garrido, J. Grandal, E. Calleja, M. A. Sánchez-Garcia, and D. López-Romero, J. Appl. Phys. **106**, 126102 (2009).
[18]C. S. Gallinat, G. Koblmüller, J. S. Brown, and J. S. Speck, J. Appl. Phys. **102**, 064907 (2007).
[19]T. Zywietz, J. Neugebauer, and M. Scheffler, Appl. Phys. Lett. **73**, 487 (1998).
[20]E. J. Tarsa, B. Heying, X. H. Hu, P. Fini, S. P. DenBaars, and J. S. Speck, J. Appl. Phys. **82**, 5472 (1997).
[21]C. Adelmann, J. Brault, D. Jalabert, P. Gentile, H. Mariette, G. Mula, and B. Daudin, J. Appl. Phys. **91**, 9638 (2002).
[22]D. Cherns, S. J. Henley, and F. A. Ponce, Appl. Phys. Lett. **78**, 18 (2001).
[23]A. E. Romanov, T. J. Baker, S. Nakamura, and J. S. Speck, J. Appl. Phys. **100**, 023522 (2006).
[24]P. Lefebvre, A. Morel, M. Gallart, T. Taliercio, J. Allègre, B. Gil, H. Mathieu, B. Damilano, N. Grandjean, and J. Massies, Appl. Phys. Lett. **78**, 1252 (2001).